

https://dspace.org/

The modelling and optimisation of aggregate plants, and the use of the Apollo Computer Program

Hayden, John Samuel

2015-01-26
http://hdl.handle.net/10539/16746

Downloaded from a DSpace repository. https://dspace.org/

So, how do crusher-output size-distributions compare with the normal distribution?

Empirical evidence obtained by the author, using a laboratory crusher, suggests that when a crusher is fed at a very **slow rate**, the resulting size distribution is essentially normal, but skewed slightly towards the fines. The mean size tends to be somewhat larger than the gap setting (by about one standard deviation).

Under **choke-fed** conditions, the size distribution is still normal on the coarse side of the mean, with a disproportionately large amount of fines, to the left of the mean. The mean of the normal component tends to approximate the gap setting.

These observations are summarised graphically in Figure 3.4.

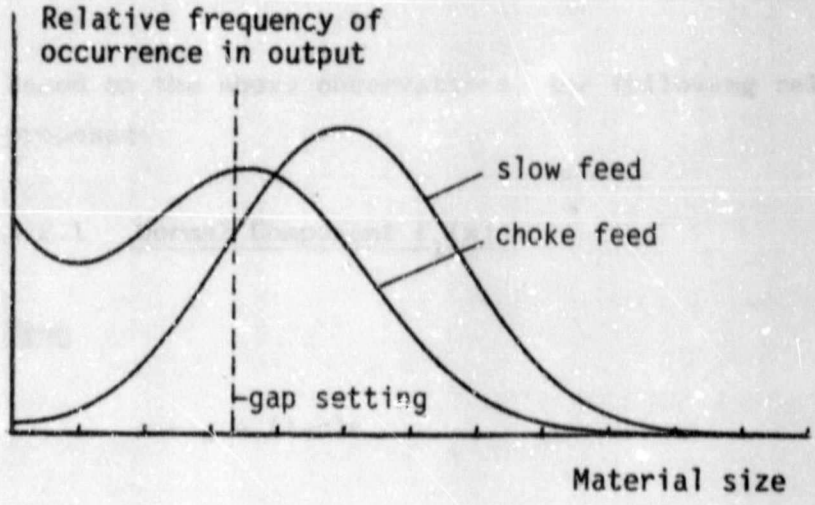


Figure 3.4 Observable characteristics of crusher-output size-distributions

Two components of the output size-distribution are thus evident: one described by a normal distribution, and the other by what can be labelled a 'fines function', whose influence depends on the feed rate. It is useful to consider that these two components are due to two separate modes of breakage in the crusher (as suggested by Whiten - see Section 3.3).

- In the first mode, particles are caught between the liners of the crusher and catastrophically fracture into a small number of relatively large particles, normally distributed in size.

- The second mode of breakage is the production of fines caused by abrasion and chipping (i.e. attrition) of particles against each other and the liners of the crusher. This mode of breakage is significant under choke loading.

The shift of the mean size to the left under choke loading, as indicated in Figure 3.4, is due to the particles remaining in the chamber for a longer time and receiving more crushing blows than would occur under slow loading.

Another observation of relevance is that as the gap setting increases, so does the standard deviation of the normal component.

Based on the above observations, the following relationships were proposed:

3.2.1 Normal Component $f_1(x)$

Mean

$$m = g + (1-r)s$$

where g = crusher gap setting
s = standard deviation
r = rate of feed, $0 < r < 1$

The relationship suggests that under choke-load conditions ($r = 1$), the mean is the same as the gap setting, and under slow-load conditions (in the limit, $r \to 0$), the mean is larger than the gap setting by one standard deviation.

Standard Deviation

It was suggested that as the gap, g, decreased to zero, so does the standard deviation, s, as shown in Figure 3.5. A relationship was accordingly proposed, of the form

$$s = \beta . g^{\delta}$$

where β and δ are constant parameters that are empirically determined for a particular crusher, by analysing the actual output gradings obtained at two different gap settings. If the gaps and standard deviations are as shown in Figure 3.5, it can be shown that $\beta = 2.523$ and $\delta = 0.263$.

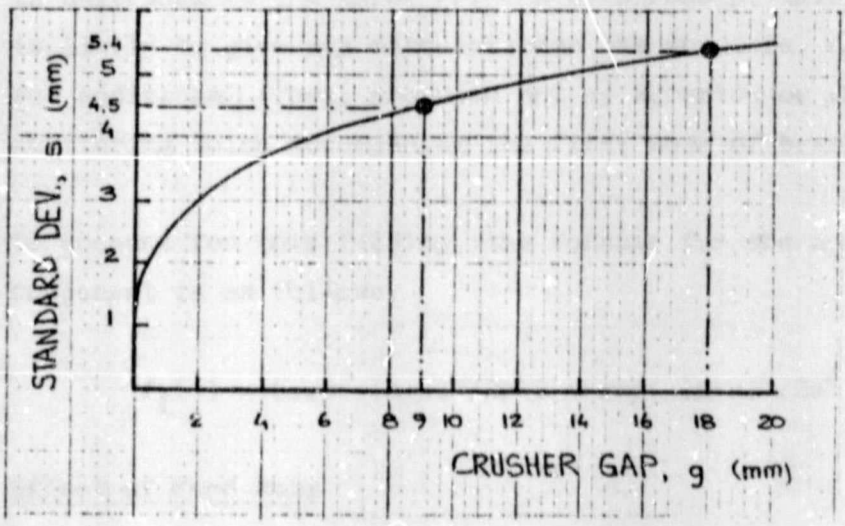


Figure 3.5 Empirical relationship between crusher gap and standard deviation for a laboratory crusher

Unity Area Considerations

The limits of the normal distribution pdf are $-\infty$ and $+\infty$, so that some of the area under the curve always falls on the negative side of the x-axis. Since particles cannot have a negative size, an adjustment is necessary.

Merely ignoring the negative part of the curve is not ideal, since the unity area under the normal curve is disturbed. What was proposed was that the negative area be 'folded' about the y-axis and added to the positive area, as shown in Figure 3.6.

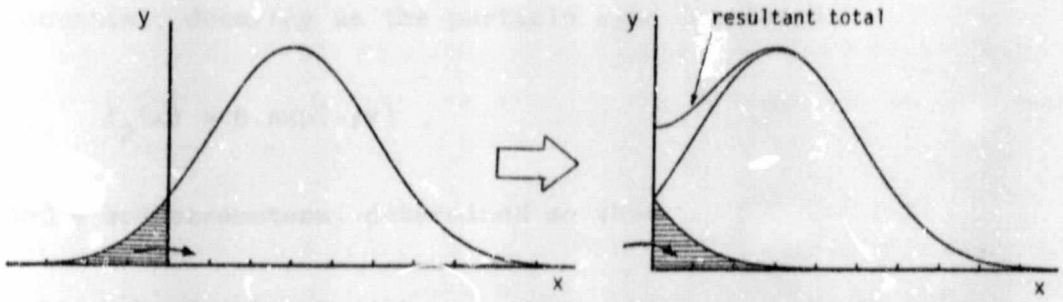


Figure 3.. 'Folding' the normal curve about the y-axis

In deference to the three Princes of Serendip, this folding, which is likely to give any mathematician the shudders, neatly accounts for additional fines, produced not by abrasion or chipping, but by shattering which accompanies the first mode of breakage.

To account for this folding, the formula for the normal distribution component is as follows:

$$f_1(x) = [\exp(-(m-x)^2/2s^2) + \exp(-(m+x)^2/2s^2)] \;/\; s\sqrt{2\pi}$$

Effect of Feed Rate

With a slow feed-rate (in the limit, r→0), the output is almost entirely due to the first breakage-mode, represented by the normal-distribution component, $f_1(x)$.

Under choke loading (r = 1), a significant proportion of the total output, say α, is due to the second mode of breakage, represented by the fines function, $f_2(x)$. Under choke-load conditions, α is typically in the range 20-30%.

The probability of occurrence of size x in the output is thus

$$f(x) = (1-\alpha r).f_1(x) + (\alpha r).f_2(x)$$

3.2.2 Fines-Function Component $f_2(x)$

It was suggested that a suitable form for the fines function was exponential, decaying as the particle size increased:

$$f_2(x) = \theta.\exp(-\phi x)$$

θ and ϕ are parameters, determined so that

when $x = 0$, $f_2(x) = \theta$

when x = gap setting (g), the curve must have decayed to, say, $\theta/10$

It can be shown that $\phi = \ln(10)/g$, so that

$$f_2(x) = \theta.\exp(-\ln(10).x/g)$$

Taking the area under the fines function curve to be unity, it follows that

$$\int_0^\infty f_2(x).dx = \int_0^\infty \theta.\exp(-\ln(10).x/g).dx = 1$$

Integrating yields $\theta = \ln(10)/g$, so that

$$f_2(x) = \ln(10).\exp[-\ln(10).x/g] \;/\; g$$

In summary, then, the relative frequency of occurrence of size x in the output is given by

$$f(x) = (1-\alpha r).f_1(x) + (\alpha r).f_2(x)$$

where $f_1(x) = [\exp(-(m-x)^2/2s^2) + \exp(-(m+x)^2/2s^2)] \;/\; s\sqrt{2\pi}$

$m = g + (1-r)s$

$s = \beta.g^{\gamma}$

$f_2(x) = \ln(10).\exp[-\ln(10).x/g] \;/\; g$

The 'cumulative percent passing size a' is given by the integral

$$F(a) = (1-\alpha r)\int_0^a f_1(x).dx + (\alpha r)\int_0^a f_2(x).dx$$

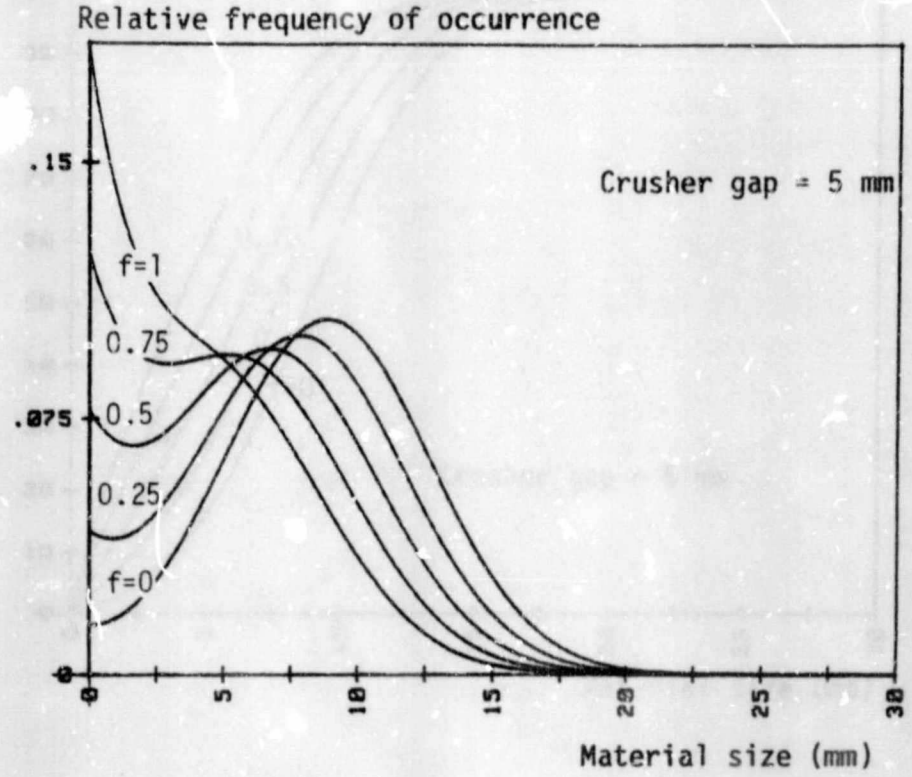
And the proportion of the output found in any size fraction, say in the interval 6.7-9.5 mm, is given by F(a), integrating between the particular size-interval limits.

Direct integration of f(x) is not possible, because of the normal component, and a numeric integration technique, such as Simpson's Rule, has to be used.

The only parameters that need to be obtained in order to use this model are α, β and δ. The first parameter, α, which describes the proportion of the output due to the fines function, is easily determined: as the feed rate varies between 0 and 1, the area under the fines-function curve increases, and the area under the normal curve decreases. This yields a proportional decrease in the height of the normal-curve mode, which can be measured. The other two parameters, β and δ, relate the standard deviation to the crusher setting: the simple empirical procedure for determining these two parameters has already been described.

The accuracy of the model in predicting output size-distribution has not been examined in too much detail, but it seems reasonable. The most important use of this model, as far as this report is concerned, is in providing a visual picture of how feed rate and crusher setting affect size distribution. Figures 3.7, 3.8 and 3.9 show the relationships that were obtained for a laboratory crusher, for which the relevant parameters were determined to be: $\alpha = 0.25$, $\beta = 2.523$ and $\delta = 0.263$.

Important to note that, like the Apollo model of a crusher, this model assumes the output grading to be independent of the feed size.



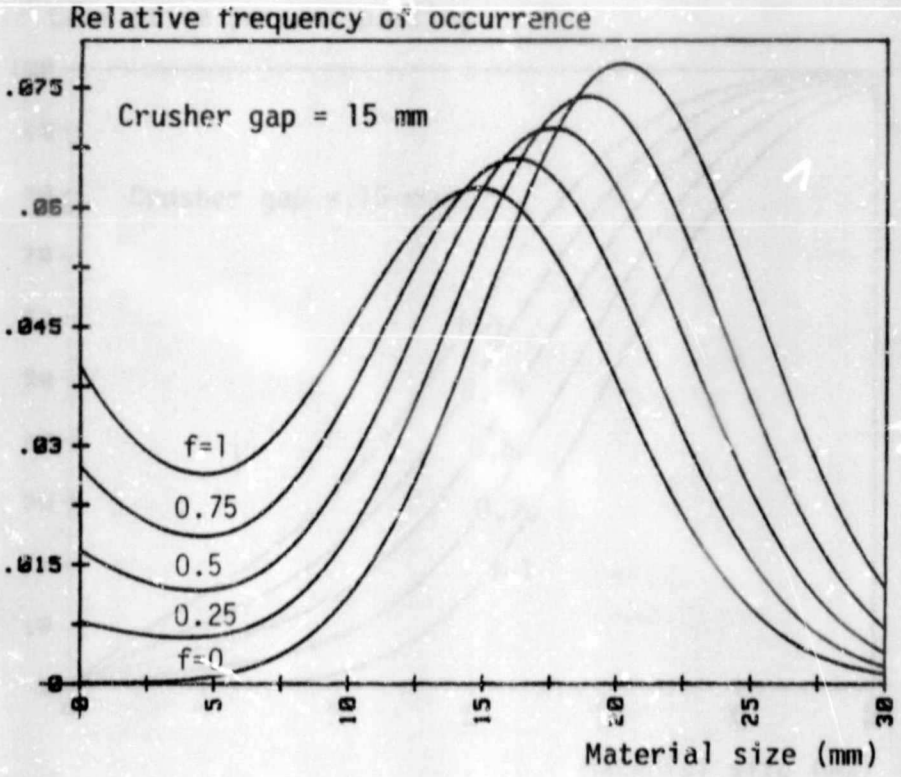
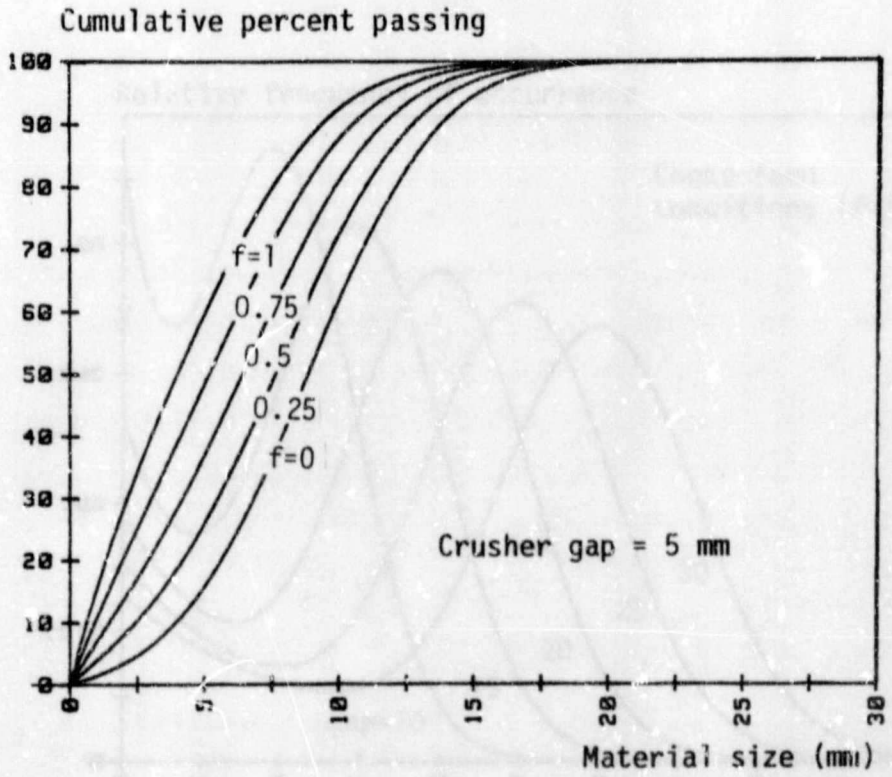


Figure 3.7 Effect of feed rate on size distribution, for two gap settings of a laboratory crusher. The graphs show the **relative frequency of occurrence** of size x in the output



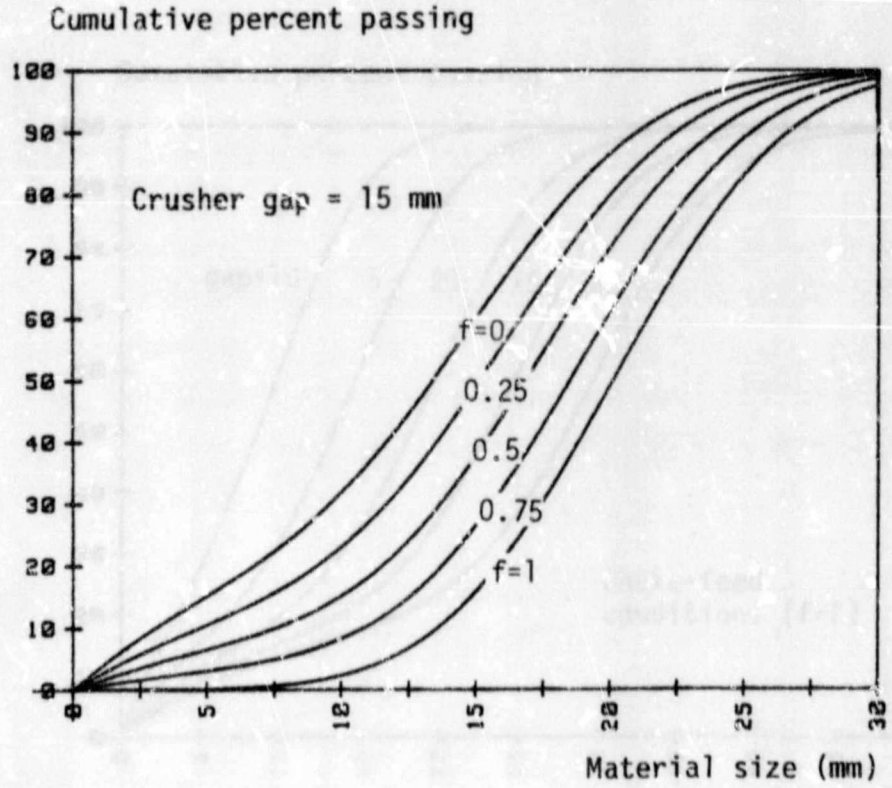


Figure 3.8 **Effect of feed rate** on size distribution, for two gap settings of a laboratory crusher. The graphs show the **cumulative percent passing** size x in the output

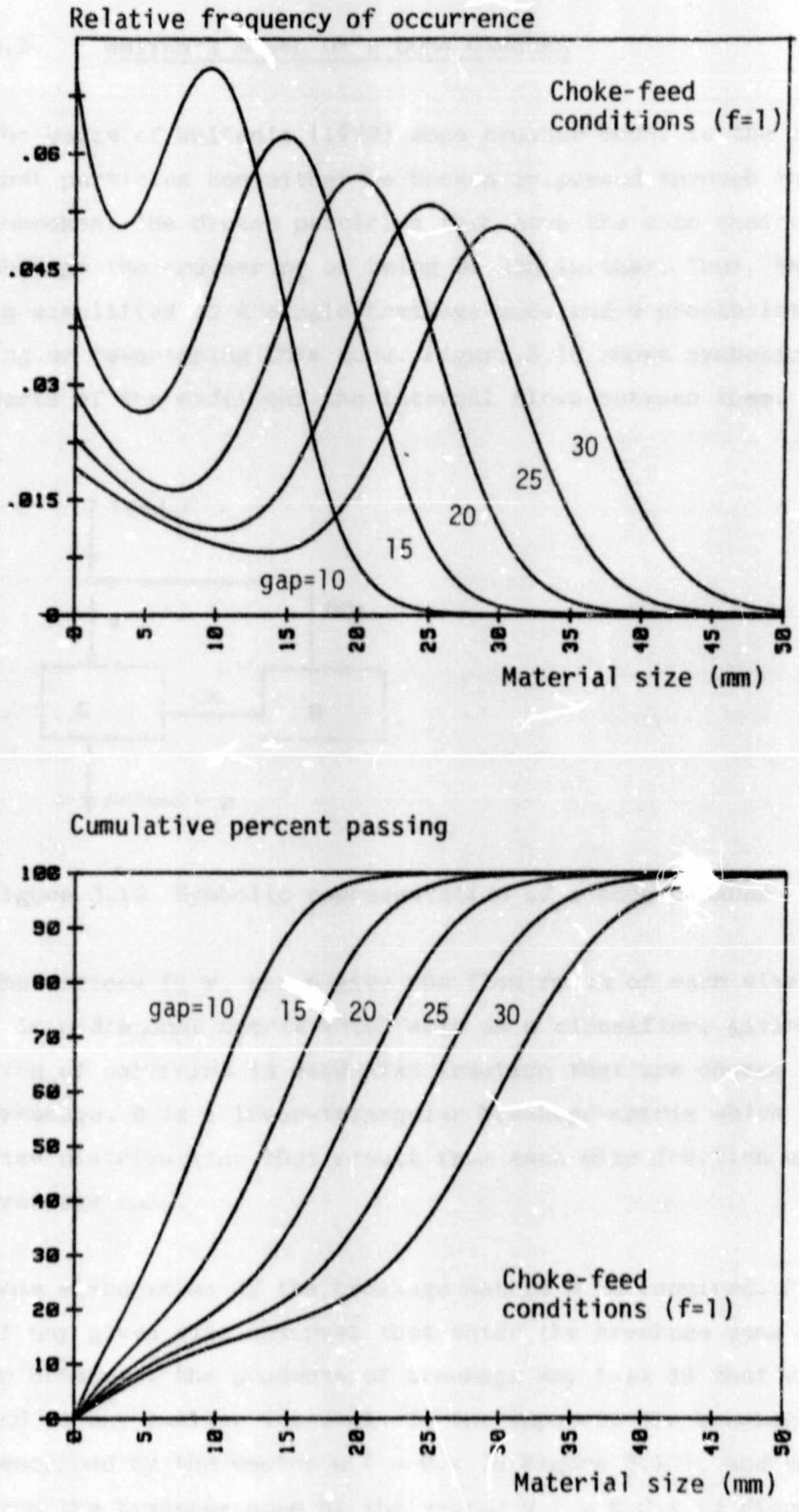


Figure 3.9 Effecty of crusher gap setting on size distribution for a laboratory crusher, showing both the relative frequency of occurrence of size x in the output, and the cumulative percent passing size x

3.3 WHITEN'S MODEL OF A CONE CRUSHER

The basis of Whiten's (1972) cone crusher model is the assumption that particles can either be broken or passed through the crusher unbroken. The broken particles then have the same choice of passing through the crusher or of being broken further. Thus, the cone crusher is simplified to a single breakage-zone and a probability of entering or re-entering this zone. Figure 3.10 shows symbolically the parts of the model and the internal flows between them.

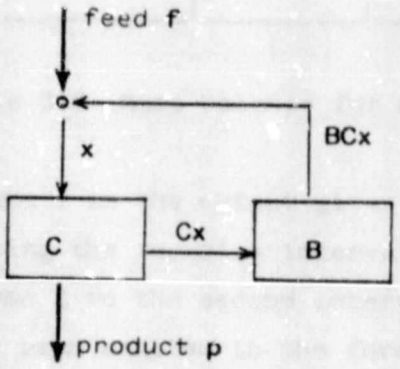


Figure 3.10 Symbolic representation of a cone crusher

The vectors **f**, **x**, and **p** give the flow rates of each size fraction. **C** is a diagonal matrix which acts as a classifier, giving the proportion of particles in each size fraction that are chosen for re-breakage. **B** is a lower-triangular breakage-matrix which gives the size distributions that result from each size fraction entering the breakage zone.

Some elaboration of the breakage matrix **B** is required. Particles of any given size interval that enter the breakage zone are subject to breakage: the products of breakage may fall in that size interval and in any smaller interval. If the input to the breakage zone is described by the vector **u** (= **C.x** in Figure 3.10), and the output from the breakage zone by the vector **v** (= **B.C.x** in Figure 3.10), then a mass balance of the breakage process can be drawn up as shown in Table 3.2.

Size interval	Input **u**	Output **v**				
1	u_1	v_{11}	0	0	..	0
2	u_2	v_{21}	v_{22}	0	..	0
3	u_3	v_{31}	v_{32}	v_{33}	..	0
.	.	.	.	.	..	.
.	.	.	.	.	..	.
n	u_n	v_{n1}	v_{n2}	v_{n3}	..	v_{nn}

Table 3.2 Mass balance for a breakage zone

Colum[illegible]utput gives the size distribution that results from passi[illegible]-size interval of the input through the breakage z[illegible] column 2 to the second interval, etc. The elements in the output have been written in the form v_{ij} where i gives the size interval in which the output element occurs and j refers to the input-particle size.

Note that interval n (the residue) can always be calculated by subtracting the cumulative amount in the other intervals from the total mass, so that the size-distribution vectors in the model are in fact adequately described by n-1 elements.

The elements v_{ij} in the array in Table 3.2 may also be written

$$v_{ij} = B_{ij}.u_j$$

where B_{ij} represents the fraction of input particles of size j which break into output particles of size i. Substituting in the array and letting $v_i = v_{i1} + v_{i2} + \ldots + v_{in}$ gives the simple matrix equation

$$\mathbf{v} = \mathbf{B}.\mathbf{u} \quad (= \mathbf{B}.\mathbf{C}.\mathbf{x} \text{ since } \mathbf{u} = \mathbf{C}.\mathbf{x})$$

The breakage matrix **B** thus transforms an input vector **u** into an output vector **v**.

What is required, however, is the transformation of the feed vector **f** into the product vector **p**. This is obtained from mass balances at the nodes in Figure 3.10, giving the equations

$$\mathbf{f} + \mathbf{B}.\mathbf{c}.\mathbf{x} = \mathbf{x}$$

and

$$\mathbf{x} = \mathbf{c}.\mathbf{x} + \mathbf{p}$$

Eliminating the internal flow **x** gives

$$\mathbf{p} = [\mathbf{I}-\mathbf{C}].[\mathbf{I}-\mathbf{B}.\mathbf{C}]^{-1}.\mathbf{f} = \mathbf{Z}.\mathbf{f} \qquad (3.1)$$

which expresses the crusher product in terms of the feed. (I is the identity matrix). The expression is a complete definition of the crushing process, but is of course only useful if the components of the transformation matrix $\mathbf{Z} = [\mathbf{I}-\mathbf{C}].[\mathbf{I}-\mathbf{B}.\mathbf{C}]^{-1}$ are known. These components are now considered.

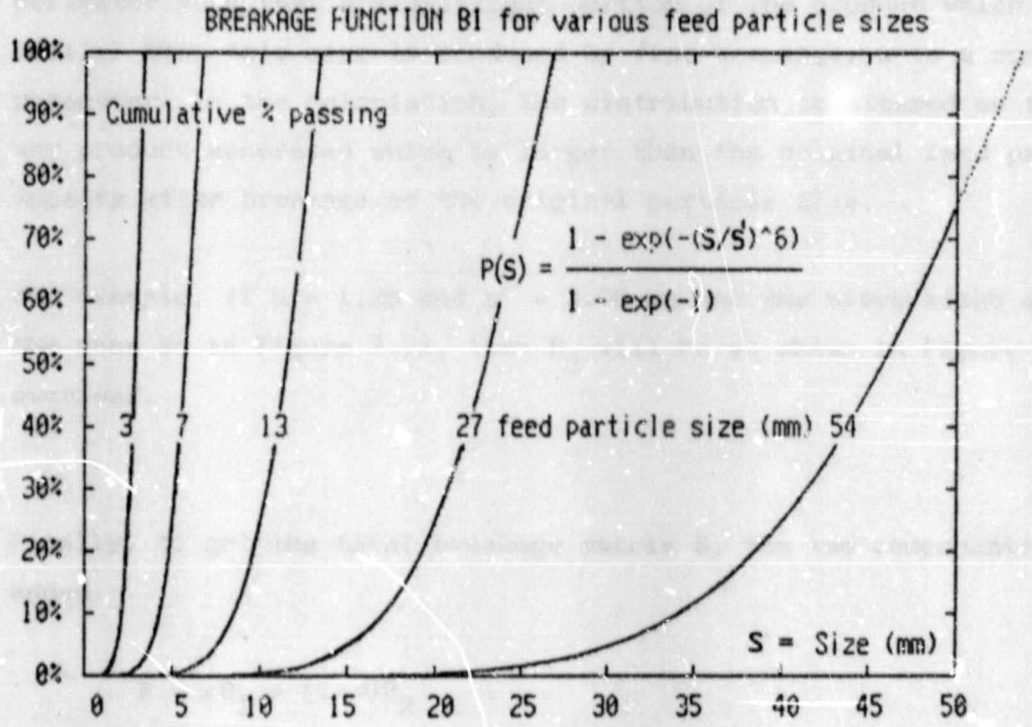
3.3.1 The Breakage Matrix B

Whiten suggested that for a cone crusher, the breakage matrix **B** consists of two parts, reflecting two modes of breakage. In the first mode, particles are caught between the liners of the crusher and catastrophically fracture into a small number of relatively large particles. This is represented by a lower-triangular matrix $\mathbf{B}_1$ which gives the product size-distribution relative to the original particle. It is calculated from:

$$p(s) = \frac{1 - \exp[-(s/s')^u]}{1 - \exp[-1]}$$

where s' is the size of the feed particle, p(s) is the cumulative percent of product smaller than size s, and u is a constant parameter. The distribution is a modification of the Rosin-Rammler distribution given by Broadbent et al (1956).

For example, if u = 6.0 and the screens used to define the size intervals are as shown in Figure 3.11, then the matrix B_1 will be as indicated in the same figure. Note that the screen sizes chosen form a constant ratio, facilitating calculations. Note also that the size of any feed particle is taken as the geometric mean of the two size limits of that interval.



level	retaining sieve	average feed-size retained	Breakage matrix B_1
(0)	(76.0mm)		
1	38.0	53.74mm	
2	19.0	26.87	
3	9.5	13.44	
4	4.75	6.72	
5	2.375	3.36	
6	0.0		

$$\begin{bmatrix} .814 & - & - & - & - \\ .183 & .814 & - & - & - \\ .003 & .183 & .814 & - & - \\ .000 & .003 & .183 & .814 & - \\ .000 & .000 & .003 & .183 & .814 \\ \hline .000 & .000 & .000 & .003 & .186 \end{bmatrix}$$

Figure 3.11 Example of breakage matrix B_1

The second mode of breakage, described by the matrix $\mathbf{B}_2$, is the production of fines caused by abrasion and chipping of particles against each other and the liners of the crusher. The sizing of this portion of the product is independent of the feed size-distribution. A Rosin-Rammler distribution is used to describe this material:

$$p(s) = 1 - \exp[-(s/s'')^u]$$

p(s) gives the cumulative percent passing size s; s'' is a fixed-size parameter such that a significant portion of the product which is smaller than this size is produced by fine breakage. u is a constant parameter. In the calculation, the distribution is altered so that any product generated which is larger than the original feed particle appears after breakage at the original particle size.

For example, if u = 1.25 and s'' = 3.05 mm and the sieve sizes are the same as in Figure 3.11, then $\mathbf{B}_2$ will be as shown in Figure 3.12, overleaf.

Finally, to get the total breakage matrix **B**, the two components are added.

$$\mathbf{B} = \alpha\mathbf{B}_1 + (1-\alpha)\mathbf{B}_2$$

where α (usually in the range 0.80 - 0.95) is a parameter related to gap size: the smaller the gap, the more fines produced.

3.3.2 The Classification Matrix C

The elements of the diagonal matrix C are obtained from a function of particle size, c(s), which gives the probability of a particle of size s entering the breakage zone. It is assumed that particles below a certain size k_1 are passed out of the crusher without further breakage, so that

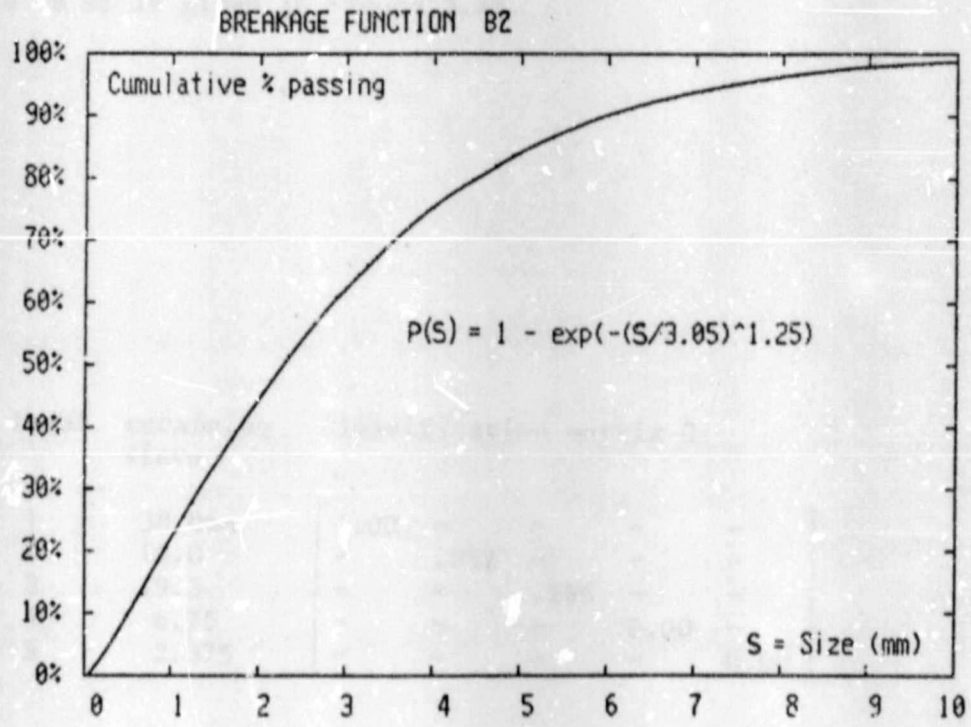
$$c(s) = 0 \quad \text{for } s < k_1$$

Also, there exists a size k_2 above which particles are always broken, so that

$$c(s) = 1 \quad \text{for } s > k_2$$

Between these sizes c(s) is assumed to be parabolic with zero gradient at k_2, so that

$$c(s) = 1 - (s-k_2)^2 / (k_1-k_2)^2 \qquad \text{for } k_1 < s < k_2$$



level	retaining sieve	Breakage matrix B_2				
(0)	(76.0mm)					
1	38.0	-	-	-	-	-
2	19.0	-	-	-	-	-
3	9.5	.016	.016	.016	-	-
4	4.75	.160	.160	.160	.176	-
5	2.375	.306	.306	.306	.306	.482
6	0.0	.518	.518	.518	.518	.518

Figure 3.12 Example of breakage matrix B_2

The elements in the C matrix are obtained as the mean values of c(s) in the appropriate size range. For the range s_1 to s_2, the matrix element is

$$\int_{s_1}^{s_2} \frac{c(s)ds}{s_2-s_1}$$

The two parameters k_1 and k_2 are related primarily to the gap and the feed tonnage.

An example of a classification matrix, assuming k_1 = 9.5 mm and k_2 = 38 mm is given in Figure 3.13.

level	retaining sieve	Classification matrix C				
1	38.0mm	1.00	-	-	-	-
2	19.0	-	.852	-	-	-
3	9.5	-	-	.296	-	-
4	4.75	-	-	-	0.00	-
5	2.375	-	-	-	-	0.00

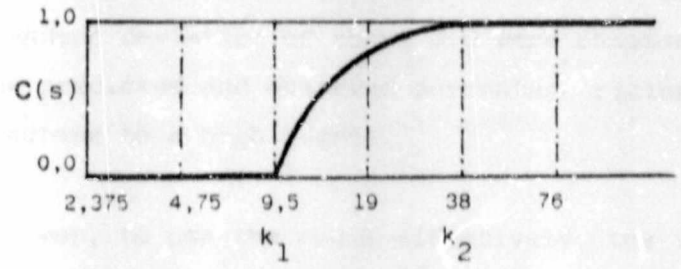


Figure 3.13 Example of classification matrix C

The elements in the C matrix are obtained as the mean values of c(s) in the appropriate size range. For the range s_1 to s_2, the matrix element is

$$\int_{s_1}^{s_2} \frac{c(s)ds}{s_2-s_1}$$

The two parameters k_1 and k_2 are related primarily to the gap and the feed tonnage.

An example of a classification matrix, assuming k_1 = 9.5 mm and k_2 = 38 mm is given in Figure 3.13.

level	retaining sieve	Classification matrix C				
1	38.0mm	1.00	-	-	-	-
2	19.0	-	.852	-	-	-
3	9.5	-	-	.296	-	-
4	4.75	-	-	-	0.00	-
5	2.375	-	-	-	-	0.00

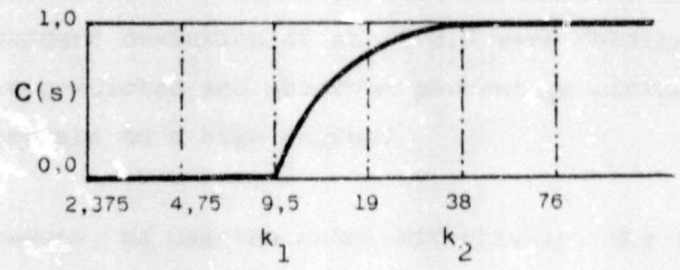


Figure 3.13 Example of classification matrix C

Having ascertained **B** and **C**, the transformation described in equation 3.1 can be determined - the equation is repeated here:

$$\mathbf{p} = [\mathbf{I}-\mathbf{C}].[\mathbf{I}-\mathbf{B}.\mathbf{C}]^{-1}.\mathbf{f}$$

Continuing the example discussed in this section, it can be shown that if the parameter α = 0.85, then the transformation matrix **Z** = $[\mathbf{I}-\mathbf{C}].[\mathbf{I}-\mathbf{B}.\mathbf{C}]^{-1}$ is as shown in Figure 3.14.

$$\begin{bmatrix} 0.00 & & & & \\ .183 & .361 & & & \\ .162 & .291 & .886 & & \\ .119 & .078 & .067 & 1.00 & \\ .201 & .101 & .018 & 0.00 & 1.00 \end{bmatrix}$$

Figure 3.14 Example of transformation matrix **Z** such that **p** = **Z.f**

Determination of the transformation matrix **Z** does of course require that the inverse of [**I-B.C**] be determined. However, if the feed vector **f** is known, the product vector **p** can be determined without any inversion: the internal vector **x** is such that **x** = $[\mathbf{I}-\mathbf{B}.\mathbf{C}]^{-1}.\mathbf{f}$ so that [**I-B.C**].**x** = **f** and we can solve for **x**. Substituting **x** into equation 3.1 gives **p** = [**I-C**].**x**.

Predictions for the cone crusher model were compared by Whiten with actual data for each of a set of tests. A mean error of 0.5 and a standard deviation of about 3.0 were obtained for the different between the predicted and observed percentage sizings. The model is therefore accurate to a high degree.

However, to use the model effectively, the following parameters have to be determined for the crusher in question: u, s", v, α, k_1 and k_2. Whiten used non-linear least squares methods to calculate these parameters for each of a set of empirical tests on a particular crusher and then used multiple spline regression techniques to predict the

parameter values over all the tests. He found that all but one of the terms were linear, the remaining one (the effect of feed rate on k_2) requiring a spline function. Values for the parameters determined by Whiten for a specific crusher are given in Figure 3.15. Details of the model building and data fitting procedures used by Whiten are given in Whiten (1971a,b).

$u = 6.0$

$s'' = 3.05$ mm

$v = 1.25$

$\alpha = 0.8723 + (0.0045)g$ (g = closed side setting in mm)

$k_1 = (0.67)g$

$k_2 = (1.121)g + (58.87)q + (25.4).T(t)$

where q is the fraction plus 25.4 mm in the feed and T(t) is as is shown below.

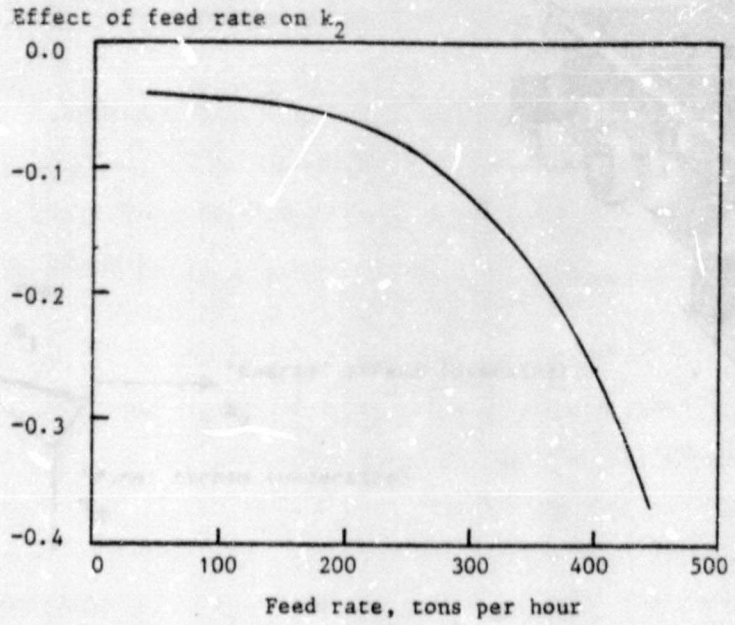


Figure 3.15 Parameters determined by Whiten for the Mount Isa Mine cone crusher, Australia

CHAPTER 4

MATHEMATICAL MODELS OF SCREENS

As was stated at the beginning of the previous chapter, the two main components of aggregate processing circuits are crushers and screens. The previous chapter dealt with the modelling of crushers; this chapter describes the mathematical modelling of screens.

A simple definition of a screen is: "a machine with a surface used to classify materials by size" (Nordberg Reference Manual, 1976). Generally, a material stream is passed over a vibrating wire mesh which serves to split it into two different size fractions as shown in Figure 4.1.

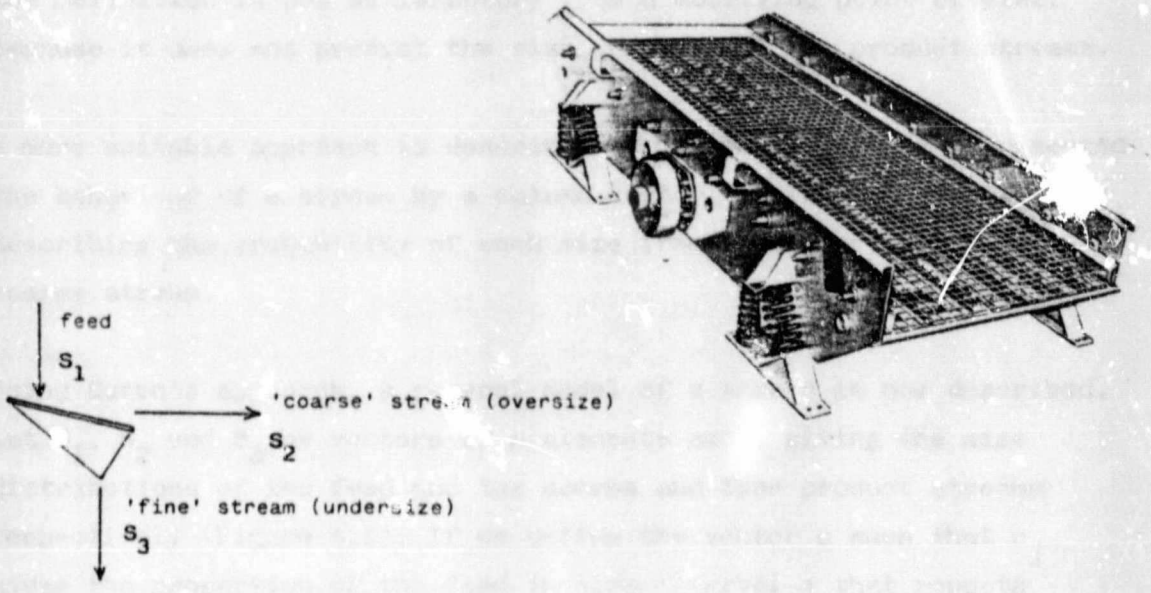


Figure 4.1 Diagramatic representation of a single-deck screen

The efficiency of a screen is determined by "how much of what should pass through the screen does pass through", or, more formally:

$$\text{Efficiency} = \frac{e-x}{e} \qquad (4.1)$$

where e is the percent undersize in the feed, and x is the percentage of the **feed** that 'wrongly' fails to pass through the surface, reporting instead to the coarse stream. It is easy to determine e, less easy to determine x, so that it is more useful to express equation 4.1 as follows:

$$\text{Efficiency}(\%) = \frac{100(e-v)}{e(100-v)} \times 100$$

where v is the percent undersize in the **coarse stream**, a more easily measured quantity than x.

It should be noted that perfect separation (100% efficiency) is not consistent with economy, and 85-95% is usually considered satisfactory.

Defining efficiency in the above manner is useful if one is determining the machine size required for a particular application, and most screen suppliers use this definition in their sizing formulae. However, the definition is not satisfactory from a modelling point of view, because it does not predict the size gradings of the product streams.

A more suitable approach is described by Gurun (1973), who represented the behaviour of a screen by a column vector, the successive elements describing the probability of each size fraction reporting to the coarse stream.

Using Gurun's approach, a general model of a screen is now described. Let $\mathbf{S_1}$, $\mathbf{S_2}$ and $\mathbf{S_3}$ be vectors of n elements each, giving the size distributions of the **feed** and the **coarse** and **fine** product streams respectively (Figure 4.1). If we define the vector **c** such that c_j gives the proportion of the feed in size-interval j that reports to the coarse stream (and $f_j = 1-c_j$ gives the fines component), then a mass balance indicates:

$$S_{2j} = S_{1j}.c_j \qquad j = 1,..,n$$

and $$S_{3j} = S_{1j}.f_j \qquad j = 1,..,n$$

In similar fashion, equations can be set up to model the double-deck screen shown in Figure 4.2.

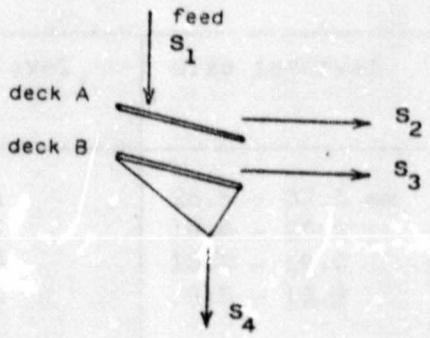


Figure 4.2 Diagramatic representation of a double-deck screen

The equations for the double-deck screen are:

$$S_{2j} = S_{1j} \cdot c_{Aj} \qquad j = 1,2,\ldots,n$$

$$S_{3j} = S_{1j} \cdot f_{Aj} \cdot c_{Bj} \qquad j = 1,2,\ldots,n$$

$$S_{4j} = S_{1j} \cdot f_{Aj} \cdot f_{Bj} \qquad j = 1,2,\ldots,n$$

The models described above are obviously only useful when predictions about screen behaviour are available and correct. In this case, the problem becomes one of determining reasonable values for the vector **c** for a particular screen surface. The elements of vector **c** can be considered as points on a continuous Efficiency Curve and various methods for determining this curve are now discussed.

4.1 PERFECT SEPARATION

Consider a screen with hole size equal to 9.5 mm, conveniently the limiting size of two adjacent size-intervals shown in Table 4.1. If perfect separation is assumed, then the vector **c**, giving the percent of each size fraction reporting to the coarse stream, is easily determined: for size fractions larger than 9.5 mm, $c_j = 100\%$, and for material smaller than 9.5 mm, $c_j = 0\%$.

level$_j$	size interval	% reporting to coarse stream (c_j)
1	26.5 - 37.5 mm	100 %
2	19.0 - 26.5	100
3	13.2 - 19.0	100
4	9.5 - 13.2	100
5	6.7 - 9.5	0
6	4.8 - 6.7	0
7	0 - 4.8	0

Table 4.1 Elements of vector **c**, assuming perfect separation

The errors incurred in assuming perfect separation are not too serious, as screening efficiencies are generally in the range 85-95%, especially in well designed plants. In fact, most aggregate plants are designed with the assumption of perfect screening incorporated into the mass flow calculations.

It is worthwhile elaborating a little on the perfect separation model, because it is, in essence, the approach used by Apollo (although with some modification, as will be explained shortly).

Continuing our example, suppose the size grading of the feed material is as shown in Table 4.2. The same table shows the gradings of the resulting coarse and fine product-streams, assuming perfect screening.

Note that there are quite a few zeros in the vectors describing the coarse and fine product-streams. Specifically, the last three elements in the coarse-stream vector, and the first four elements in the fine-stream vector, are zeros.

$level_j$	size interval	c_j	material gradings (tons)		
			feed	coarse	fine
1	26.5 - 37.5 mm	100 %	5 tons	5 tons	-
2	19.0 - 26.5	100	13	13	-
3	13.2 - 19.0	100	21	21	-
4	9.5 - 13.2	100	14	14	-
5	6.7 - 9.5	0	8	-	8 tons
6	4.8 - 6.7	0	6	-	6
7	0 - 4.8	0	33	-	33

Table 4.2 Product gradings, assuming perfect separation

In the Apollo model, these zero elements are discarded, in order to reduce the number of variables and equations generated. The coarse-stream vector would thus be represented by only 4 variables, and the fine-stream vector by only 3 variables.

4.2 PROBABILISTIC MODEL OF A VIBRATING SCREEN

A useful model for determining a realistic Efficiency Curve for a screen has been developed from simple probabilistic considerations by Whiten (1972). The parameters in the model are found by fitting the model to experimental data using least-squares methods or other data-fitting procedures.

The probability that a particle of size x does not pass through a screen with hole size h and wire diameter

$$E(x) = [1 - (h-x)^2/(h+d)^2]^m$$

Author Hayden John Samuel
Name of thesis The Modelling And Optimisation Of Aggregate Plants, And The Use Of The Apollo Computer Program. 1986

PUBLISHER:

University of the Witwatersrand, Johannesburg
©2013

LEGAL NOTICES:

Copyright Notice: All materials on the University of the Witwatersrand, Johannesburg Library website are protected by South African copyright law and may not be distributed, transmitted, displayed, or otherwise published in any format, without the prior written permission of the copyright owner.

Disclaimer and Terms of Use: Provided that you maintain all copyright and other notices contained therein, you may download material (one machine readable copy and one print copy per page) for your personal and/or educational non-commercial use only.

The University of the Witwatersrand, Johannesburg, is not responsible for any errors or omissions and excludes any and all liability for any errors in or omissions from the information on the Library website.